Electronic Supplementary Material (ESI) for ChemComm.

Supporting Information

Unique Rectilinearly π-Extended Rhodamine Dye with Large Stokes Shift and Near-Infrared Fluorescence for Bioimaging

*Chang Liu, Xiaojie Jiao, Qing Wang, Kun Huang, Song He, Liancheng Zhao and Xianshun Zeng**

Materials and instrumentation

Starting materials and reagents were purchased from Tokyo Kasei Kogyo (TCI: Tokyo, Japan), AR grade or dry grade solvents were purchased from Alfa-Aesar, and used without further purification. The reactions were carried out in oven-dried glasswares with a magnetic stirring. ER-Tracker Green, LysoTracker Green DND-26, MitoTracker Green and Golgi-Tracker Green were purchased from Beyotime Institute of Biotechnology. MTT 3-(4,5-dimethylthiazol-2-yl)-2,5-diphenyltetrazolium bromide was purchased from Sigma. NMR spectra were recorded on a Bruker spectrometer at 400 (^{1}H NMR) MHz and 100 (^{13}C NMR) MHz. Chemical shifts (d values) were reported in ppm down field from internal Me_4Si (^{1}H and ^{13}C NMR). High resolution mass spectra (HRMS) were acquired on an Agilent 6510 Q-TOF LC/MS instrument (Agilent Technologies, Palo Alto, CA) equipped with an electro-spray ionization (ESI) source. Elemental analyses were performed on a Vanio-EL elemental analyzer (Analyze-system GmbH, Germany). Melting points were recorded on a Boethius Block apparatus and uncorrected. All absorption spectra were recorded using a Shimadzu UV-2550 UV/Vis spectrophotometer with 1cm quartz cell. In a similar manner, fluorescence spectra were recorded on a Hitachi F-4600 spectrofluorophotometer with a 1 cm quartz cell. Cells imaging was performed with a Nikon Eclipse TE2000U inverted fluorescence microscopy and a confocal microscope (Olympus FV1000-IX81) with a 10 × objective lens. All images were analyzed with Olympus FV1000-ASW.

Synthesis and Compound Characterizations

The preparation of TJ730.

To a 50 mL flask, 2-(4-(diethylamino)-2-hydroxybenzoyl)benzoic acid (6.01 g, 19 mmol) and 10-ethyl-2-methoxy-10*H*-phenothiazine (5.21 g, 19 mmol) were mixed in methanesulfuric acid and heated at 70 ^{o}C for 12 h. The reaction mixture was poured into stirred ice water and its pH was adjusted to 7-8 with sodium bicarbonate aqueous solution. Then, the reaction mixture was stirred for 20 min and subsequently extracted with CH_2Cl_2 three times. The organic layers were dried over Na_2SO_4 and evaporated to give the crude product. The crude product was purified by silica gel column chromatography (DCM/ethanol, 100/2-100/10, v/v) and further recrystallized from CH_2Cl_2 solution to obtain the blue product **TJ730** in 72 % yield (7.1 g), m.p. 112-114 ^{o}C. HRMS: m/z $[M + H]^+$ = 521.1893; Calcd: 521.1897; ^{1}H NMR ($CDCl_3$, 400 MHz, ppm) 8.01 (d, *J* = 7.2 Hz, 1H), 7.65 (t, *J* = 8.0 Hz, 1H), 7.60 (t, *J* = 8.0 Hz, 1H), 7.17 (d, *J* = 7.6 Hz, 1H), 7.13 (t, *J* = 8.4 Hz, 1H), 7.03 (d, *J* = 8.0 Hz, 1H), 6.89 (t, *J* = 7.0 Hz, 2H), 6.72 (s, 1H), 6.55 (d, *J* = 8.8 Hz, 1H), 6.44 (s, 2H), 6.36 (d, *J* = 8.0 Hz, 1H), 3.95 (m, 2H, *J* = 6.8 Hz), 3.36 (m, *J* = 7.2 Hz, 4H); 1.47 (t, *J* = 6.8 Hz, 3H); 1.17 (m, *J* = 7.2 Hz, 6H); ^{13}C NMR (DMSO-d_6, 100 MHz, ppm) 158.23, 150.29, 148.47, 144.05, 131.58, 125.19, 124.62, 123.42, 123.30, 122.81, 122.36, 121.90, 120.00, 118.82, 116.73, 115.77, 113.53, 109.45, 108.69, 108.41, 107.72, 92.74, 88.33, 70.62, 70.19, 69.76, 40.45, 38.74, 36.29, 4.66.

The preparation of 2.

The crude product **TJ730** (5.0 g, 1 mmol) were refluxed in 30 mL ethanol with 8 mL concentrated sulfuric acid for 24 h. The reaction mixture was poured into stirred ice water and its

pH was adjusted to 7-8 with sodium bicarbonate aqueous solution. Then, the reaction mixture was stirred for 20 min and subsequently extracted with CH_2Cl_2 three times. The organic layers were dried over Na_2SO_4 and evaporated to give the crude product. The crude product was purified by silica gel column chromatography (DCM/ethanol, 100/2-100/25, v/v) and further recrystallized from CH_2Cl_2 solution to obtain the blue product **2** in 72 % yield (3.8 g), m.p. 128-130 ^oC. HRMS: m/z $[M+H]^+$ = 549.2206; Calcd: 549.2217; ^1H NMR ($CDCl_3$, 300 MHz, ppm) 8.31 (d, *J* = 8.0 Hz, 1H), 7.81 (t, *J* = 8.0 Hz, 1H), 7.75 (t, *J* = 8.0 Hz, 1H), 7.27 (d, *J* = 4.0 Hz, 1H), 7.24 (d, *J* = 3.2 Hz, 1H), 7.19 (t, *J* = 7.6 Hz, 1H), 7.05 (t, *J* = 7.2 Hz, 1H), 6.98 (t, *J* = 8.0 Hz, 2H), 6.66 (d, *J* = 8.0 Hz, 1H), 4.10 (m, 4H), 3.69 (m, 4H); 1.34 (s, 6H);1.25 (t, *J* = 6.8 Hz, 3H); 1.01 (m, *J* = 7.2 Hz, 3H); ^{13}C ($CDCl_3$, 75 MHz, ppm) 165.12, 158.57, 157.77, 156.97, 156.82, 152.37, 139.91, 133.49, 133.29, 131.77, 131.73, 130.89, 130.36, 128.58, 127.37, 125.19, 123.97, 123.80, 121.56, 117.50, 116.95, 116.90, 115.88, 101.35, 97.12, 63.15, 61.95, 46.92, 44.51, 15.56, 14.13, 12.54.

The preparation of 3.

To a 50 mL reactor, was charged **2** (160 mg, 0.29 mmol), phenylhydrazine (0.5 mL), ethanol (5 mL). The reaction mixture was stirred for 6 h at 60 ^oC. The reaction mixture was extracted with CH_2Cl_2 three times. The organic layers were dried over Na_2SO_4 and evaporated to give the crude product. The crude product was purified by silica gel column chromatography (DCM/ethanol, 100/2-100/7.5, v/v). **3** was obtained as yellow powder in 17% yield (30 mg); m.p. 184-186 ^oC. HRMS: m/z $[M + H]^+$ = 611.2480; Calcd: 611.2489; ^1H NMR ($CDCl_3$, 400 MHz, ppm): 8.03 (d, *J* = 8.0 Hz, 1H), 7.59 (m, *J* = 4.0 Hz, 2H), 7.21 (d, *J* = 8.0 Hz, 1H), 7.13 (t, *J* = 8.0 Hz, 1H), 7.05 (d, *J* = 8.0 Hz, 1H), 6.89 (m, *J* = 6.0 Hz, 4H), 6.61 (t, *J* = 8.0 Hz, 1H), 6.49 (t, *J* = 8.0 Hz, 4H), 6.38 (s, 1H), 6.33 (s, 2H), 5.36 (s, 1H), 3.87 (m, *J* = 8.0 Hz, 2H), 3.33 (m, *J* = 8.0 Hz, 4H), 1.40 (t, *J* = 8.0 Hz, 3H), 1.16 (t, *J* = 6.0 Hz, 6H) ; ^{13}C NMR ($CDCl_3$, 75 MHz, ppm): 166.18, 153.66, 152.60, 149.09, 146.36, 146.01, 143.66, 133.08, 130.69, 128.72, 128.16, 127.13, 125.59, 124.30, 123.97, 123.46, 122.52, 120.60, 118.81, 115.18, 114.71, 113.19, 108.86, 103.16, 66.42, 45.30, 42.75, 13.75, 13.43.

The preparation of 4.

To a 50 mL reactor, was charged **2** (150 mg, 0.27 mmol), 4-(2-hydrazinylethyl)morpholine (0.5 mL) and ethanol (5 mL). The reaction mixture was stirred for 3 h at room temperature. The reaction mixture was extracted with CH_2Cl_2 three times. The organic layers were dried over Na_2SO_4 and evaporated to give the crude product. The crude product was purified by silica gel column chromatography (DCM/ethanol, 100/2-100/10, v/v) and further recrystallized from diethyl ether. **4** was obtained as white powder in 34% yield (60 mg); m.p. 140-142 ^oC. HRMS: m/z $[M +H]^+$ = 648.3012; Calcd: 648.3003; ^1H NMR ($CDCl_3$, 400 MHz, ppm) 7.92-7.90 (m, *J* = 2.8 Hz, 1H), 7.49-7.47 (m, *J* = 2.8 Hz, 2H), 7.14 (t, *J* = 7.6 Hz, 1H), 7.05 (t, *J* = 8.0 Hz, 2H), 6.88 (t, *J* = 7.6 Hz, 2H), 6.68 (s, 2H), 6.43 (d, *J* = 8.8 Hz, 1H), 6.38 (d, *J* = 2.0 Hz, 1H), 6.35 (s, 1H), 6.30-6.27 (m, *J* = 3.6 Hz, 1H), 4.70 (s, 1H), 3.97-3.92 (m, *J* = 6.8 Hz, 2H), 3.62 (s, 4H), 3.36-3.31 (m, *J* = 6.8 Hz, 4H), 2.73 (s, 1H), 2.60 (s, 1H), 2.31 (s, 4H), 2.21 (d, *J* = 4.8 Hz, 2H), 1.47 (t, *J* = 6.8 Hz, 3H), 1.16 (t, *J* = 6.8 Hz, 6H). ^{13}C NMR ($CDCl_3$, 100 MHz, ppm) 166.67, 153.79, 152.82, 151.13, 149.15, 146.40, 144.12, 133.13, 130.72, 129.04, 128.86, 127.66, 127.61, 125.97, 124.28, 124.15, 123.15, 122.93, 118.67, 115.49, 113.91, 108.47, 105.48, 103.38, 98.02, 67.20, 65.32, 56.45, 53.48, 47.03, 44.67, 42.39, 13.10, 12.90.

Determination of the Fluorescence Quantum Yield.

Fluorescence quantum yield (Φ_1) was determined by using rhodamine B (Φ_1 = 0.71, in ethanol)[S1] as the fluorescence standard. The quantum yield was calculated using the following equation.

$$\Phi_1 = \Phi_B \times \frac{Abs_B \times F_1 \times \lambda_{exB} \times \eta_1}{Abs_1 \times F_B \times \lambda_{ex1} \times \eta_B}$$

Where Φ_1 is the fluorescence quantum yield, A is the absorbance at the excitation wavelength, F is the area under the corrected emission curve, and η is the refractive index of the solvent used. Subscripts 1 and B refer to the unknown and to the standard, respectively.

Cell Culture and Imaging Methods.

The cells were grown in RPMI 1640 supplemented with 10% FBS (fetal bovine serum) in an atmosphere of 5% CO_2 and 95% air at 37 ^oC. L929 cells and HeLa cells were planted on 24-well plates and allowed to adhere for 24 h. INS-1 cells were cultured in RPMI-1640 medium supplemented with 10% fetal bovine serum (FBS), 100 U/ml penicillin, 100 μg/ml streptomycin, 1 mmol/l sodium pyruvate, and 50 μmol/l β-mercaptoethanol. Before the experiments, the cells were washed with phosphate-buffered saline (PBS) buffer. Subsequently, the cells were incubated with dyes **TJ730**, **2** and probes **3**, **4** (containing 0.1% DMSO as a cosolvent) for 30 min at 37 ºC, and then washed with PBS three times. Fluorescence imaging experiments were performed on FV 1000-IX81 (Olympus) confocal laser scanning microscope.

MTT assay

L929 cells were seeded onto 96 well tissue culture plates in sterile conditions. After harvesting for overnight cells were incubated for 24 h in the absence or presence of different concentrations (0.1 μM - 50 μM) of **TJ730**, **2**, probes **3** and **4**. Treated cells were incubated for 4 h in presence of MTT solution prepared from 0.012 mol/L of 3-(4,5-dimethylthiazol-2-yl)-2,5-diphenyltetrazolium bromide in PBS. DMSO was used as MTT solvent and cell population was analyzed by observing absorbance at 570 nm using Biotek Epoch Microplate Reader. Data analysis was performed using following formula:

$$\% \text{ of Viable cells} = [(A_{490\,TC} - A_{490\,B})/(A_{490\,UC} - A_{490\,B})] \times 100$$

(TC-Treated cells, B-Background, UC-untreated cells)

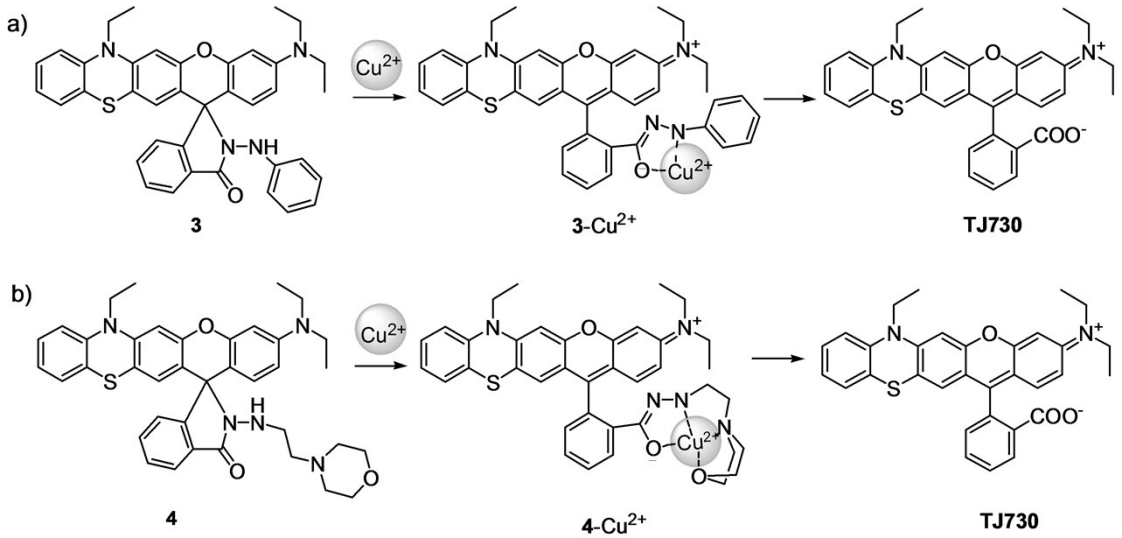

Scheme S1. Proposed reaction of **3** and **4** with Cu^{2+}.

Table S1. Photophysical properties of the dye **TJ730** in different solvents in the presence of TFA (1%).

Solvents	λ_{max} (nm)	ε ($M^{-1}cm^{-1}$)	PL_{max} (nm)	Φ	Stokes shift (nm)
acetone	606	34600	734	0.046	128
Toluene	609	64400	738	0.053	129
CHCl3	627	35700	739	0.072	112
DCM	622	34100	736	0.067	114
DMF	609	31100	738	0.031	129
DMSO	613	32400	741	0.032	128
EtOAc	610	32000	732	0.053	122
EtOH	606	33300	730	0.047	124
H2O	616	15700	738	0.002	122
MeCN	605	33700	734	0.047	129
MeOH	603	33400	730	0.032	127
THF	613	30400	735	0.045	122

Table S2. Photophysical properties of the dye **2** in different solvents.

Solvents	λ_{max} (nm)	ε ($M^{-1}cm^{-1}$)	PL_{max} (nm)	Φ	Stokes shift (nm)
acetone	610	34900	727	0.039	117
Toluene	624	33000	730	0.027	106
$CHCl_3$	622	35200	725	0.075	103
DCM	622	36400	722	0.056	100
DMF	617	35400	730	0.024	113
DMSO	617	36400	735	0.023	118
EtOAc	611	35300	720	0.039	109
EtOH	613	35100	726	0.030	113
H_2O	604	30300	727	0.005	121
MeCN	607	35100	727	0.038	120
MeOH	609	34900	725	0.022	116
THF	616	40300	727	0.031	111

Table S3. The fluorescence lifetime of **TJ730**, **2**, **3** and **4**.

	Solvent	τ (ns)
TJ730	MeCN	6.12
2	MeCN	3.09
3	MeCN	0.63
4	MeCN	3.17

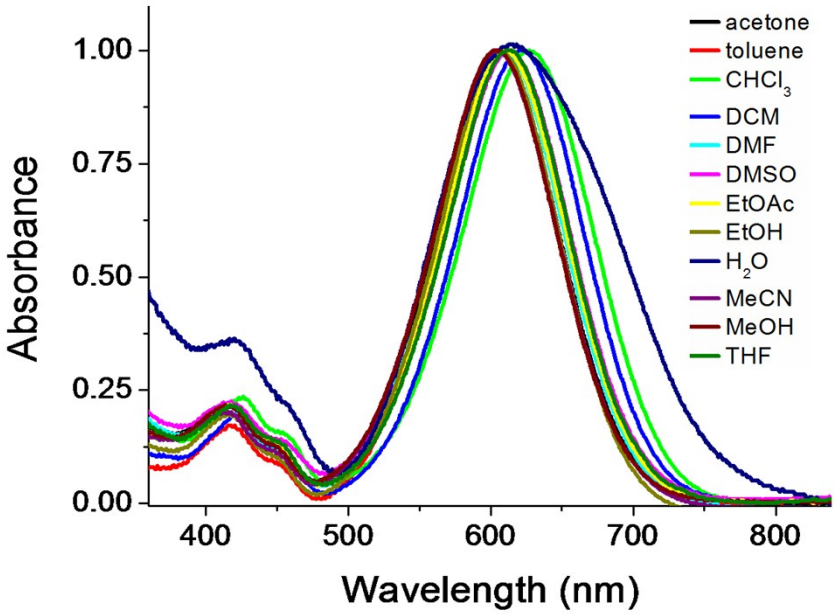

Figure S1. Absorption spectra of **TJ730** (10 μM) in different solvents in the presence of TFA (1%).

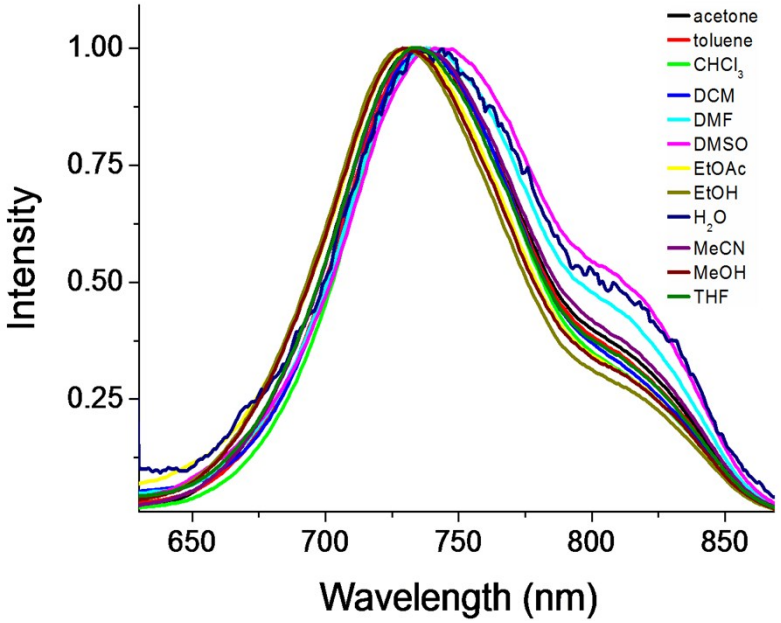

Figure S2. Fluorescence emission spectra of **TJ730** (5 μM) in different solvents in the presence of TFA (1%). λ_{ex} = 610 nm, slit: 10 nm, 10 nm.

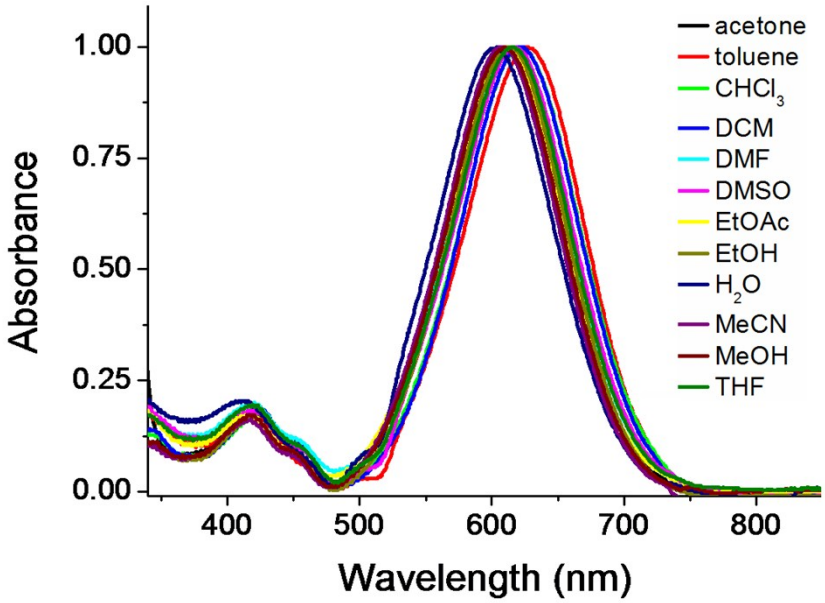

Figure S3. Absorption spectra of **2** (10 μM) in different solvents.

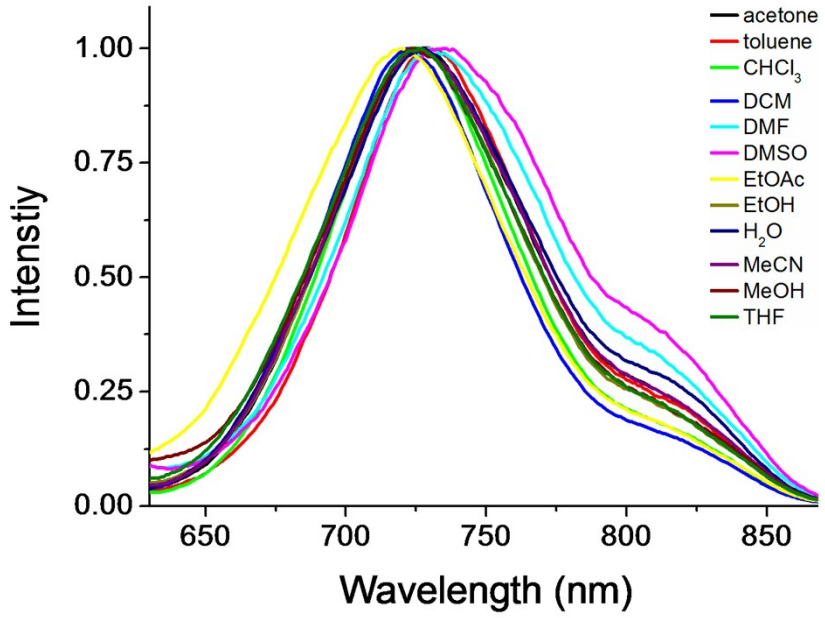

Figure S4. Fluorescence emission spectra of **2** (5 μM) in different solvents. λ_{ex} = 610 nm, slit: 10 nm, 10 nm.

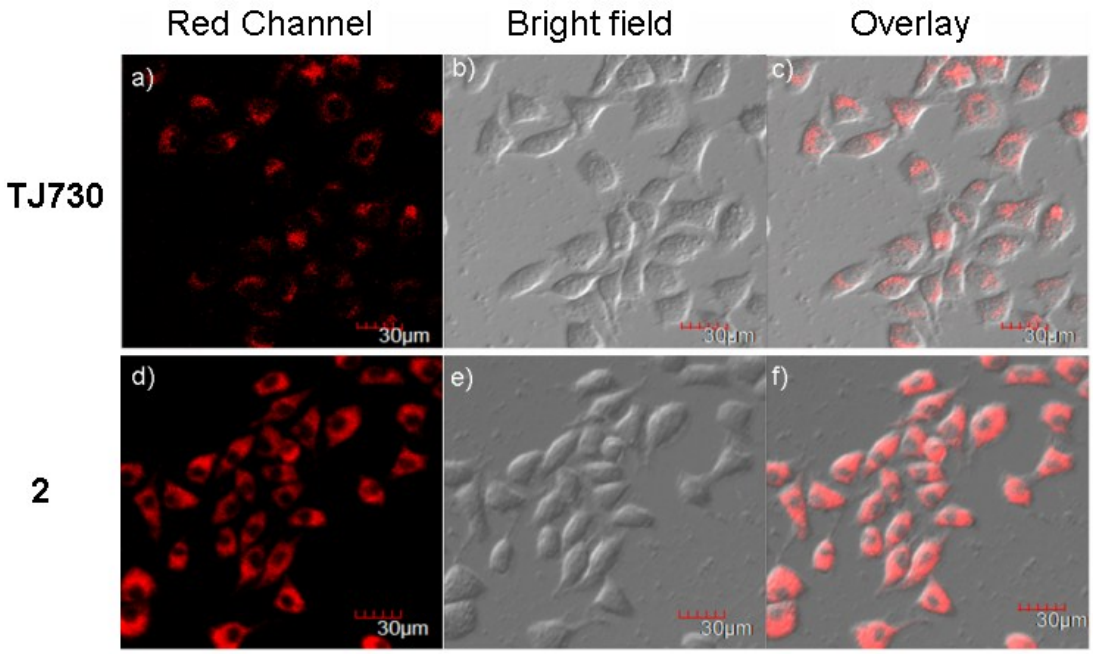

Figure S5. Fluorescence image of L929 cells incubated with the dye **TJ730** (1 μM) and **2** (1 μM). a), d) fluorescence image after staining for 30 min; b), e) brightfield image after staining for 30 min; c) the overlay a) and c); f) the overlay d) and e). λ_{ex} = 635 nm, λ_{em}: 650-750 nm

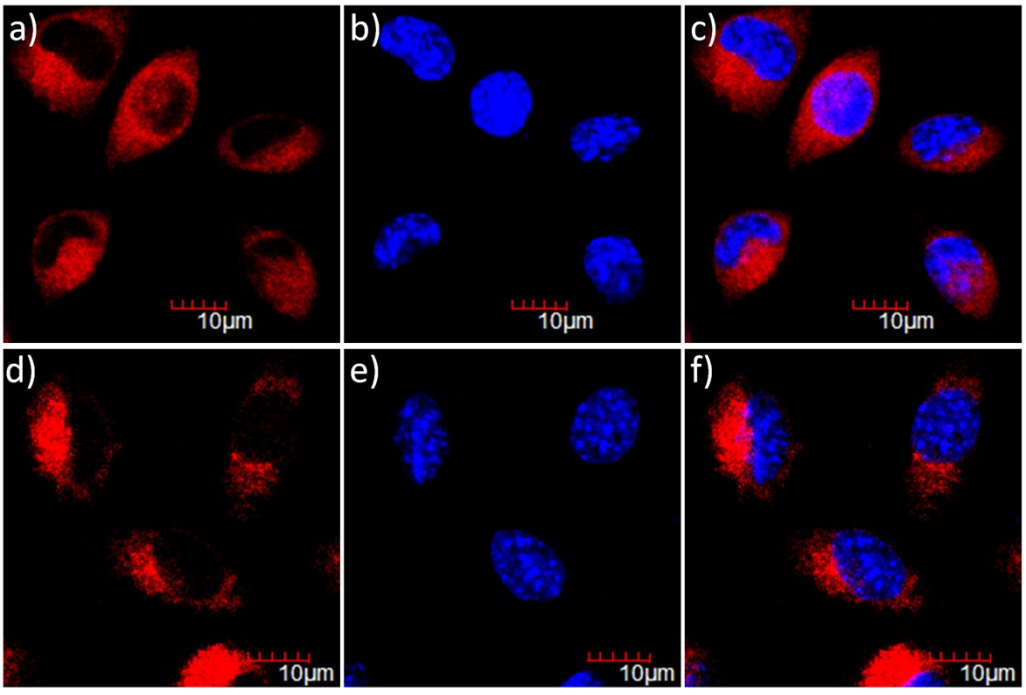

Figure S6. Fluorescence image of L929 cells incubated with DAPI and **TJ730** (a-c), and DAPI with **2** (d-f). L929 cells loaded with DAPI (0.36 μM) for 12 h, **TJ730** or **2** (1 μM) were loaded into L929 cells for 30 min. (a, d) Fluorescence image of **TJ730** and **2** (λ_{ex} = 635 nm, λ_{em}: 650-750 nm); (b, e) Fluorescence image of DAPI (λ_{ex} = 405 nm, λ_{em}: 425-475 nm); (c, f) Merged images of DAPI with **TJ730** and **2**.

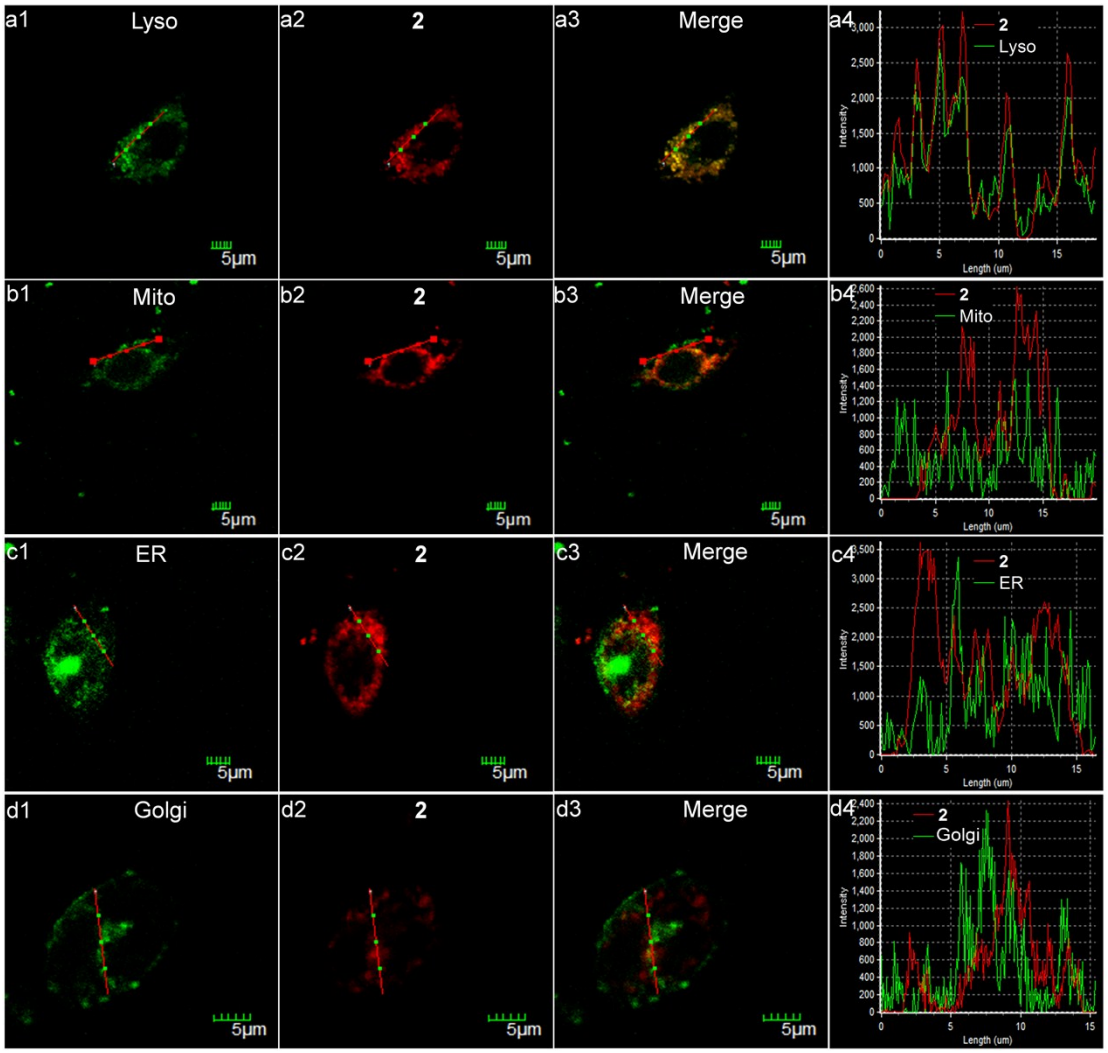

Figure S7. Fluorescence imaging of HeLa cells costained with **2** (1 μM) and Lyso Tracker Green (200 nM), MitoTracker Green (200 nM), Golgi-Tracker (200 nM), or ER-Tracker (200 nM). Cells were incubated with dyes at 37 °C for 30 min in serum-free medium, and then washed before confocal imaging. Probes are indicated on each fluorescent image. Plots in the last column represent the intensity profiles of respective probe with 2 within the linear ROIs across the HeLa cell.

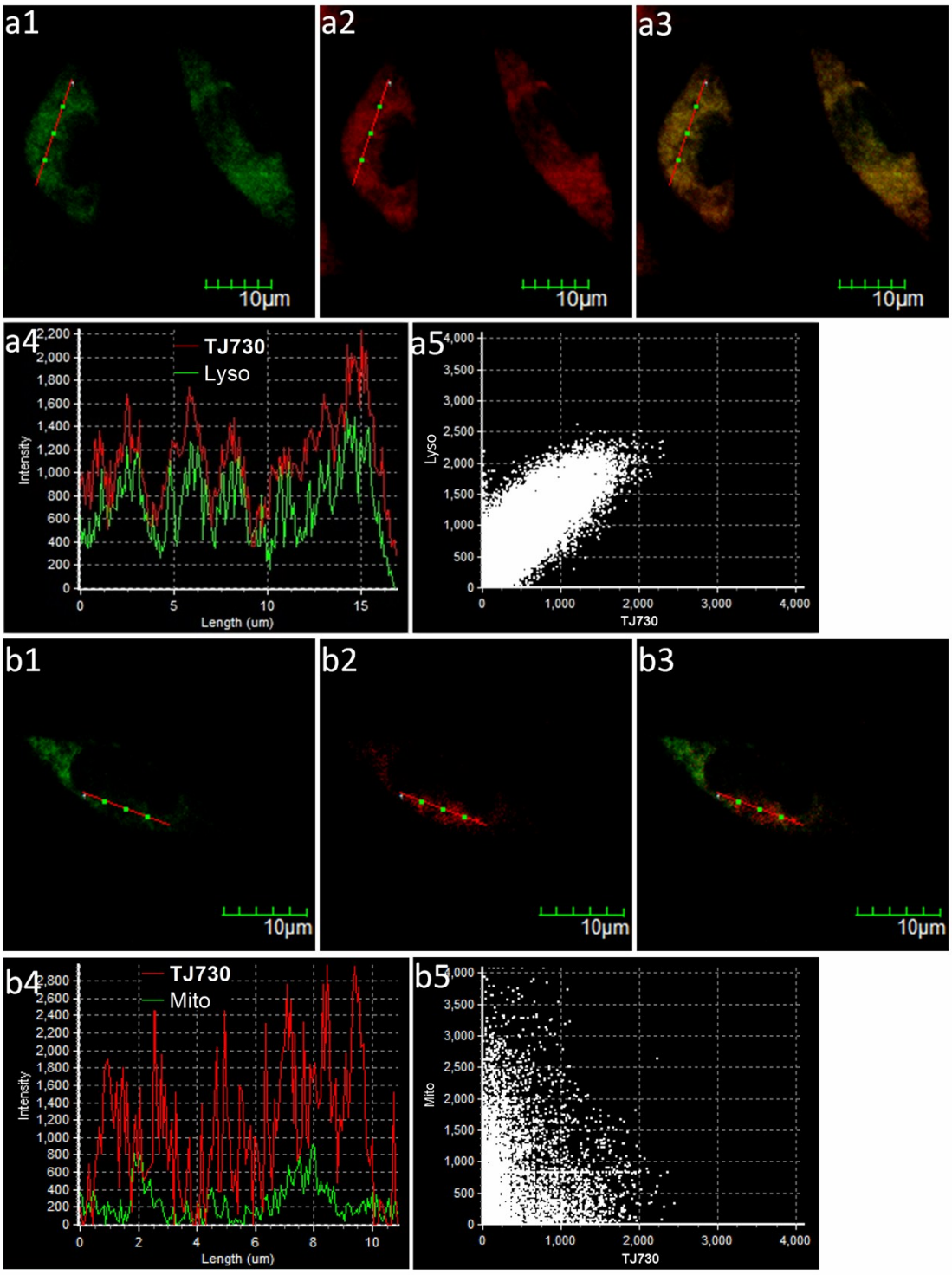

Figure S8. Localization of **TJ730** in lysosome in L929 cells. LysoTracker Green (100 nM), Mito tracker (100 nM) and **TJ730** (500 nM) were loaded into L929 cells for 30 min, respectively. (a1, b1) Fluorescence image of LysoTracker Green and Mito tracker, respectively. (a2, b2) Fluorescence image of **TJ730**. (a3, b3) Merged images of LysoTracker Green and Mito tracker with **TJ730**, respectively. (a4, b4) Intensity profiles of LysoTracker Green and Mito tracker with **TJ730** within the linear ROIs (red lines in cells) across the L929 cell, respectively. (a5, b5) Intensity correlation plot of LysoTracker Green and Mito tracker with **TJ730**, respectively.

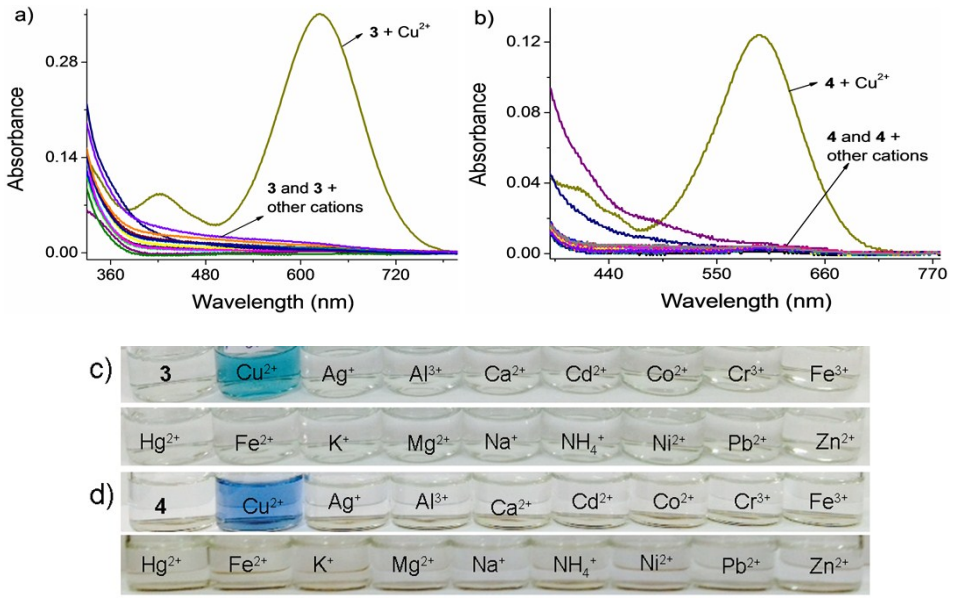

Figure S9. a) and b) Absorbance spectra of **3** and **4** (10 μM) upon the addition of the nitrate salts (5.0 equiv.) of Ag^{+}, Al^{3+}, Ca^{2+}, Cd^{2+}, Co^{2+}, Cr^{3+}, Fe^{3+}, Hg^{2+}, K^{+}, Mg^{2+}, Na^{+}, NH_4^{+}, Ni^{2+}, Pb^{2+}, $Zn^{2+}$and Cu^{2+} in H_2O-MeCN (2:1, v/v). c) and d) Color changes of **3** and **4** (10 μM) in the presence of 5.0 equiv of various ions in H_2O-MeCN (2:1, v/v).

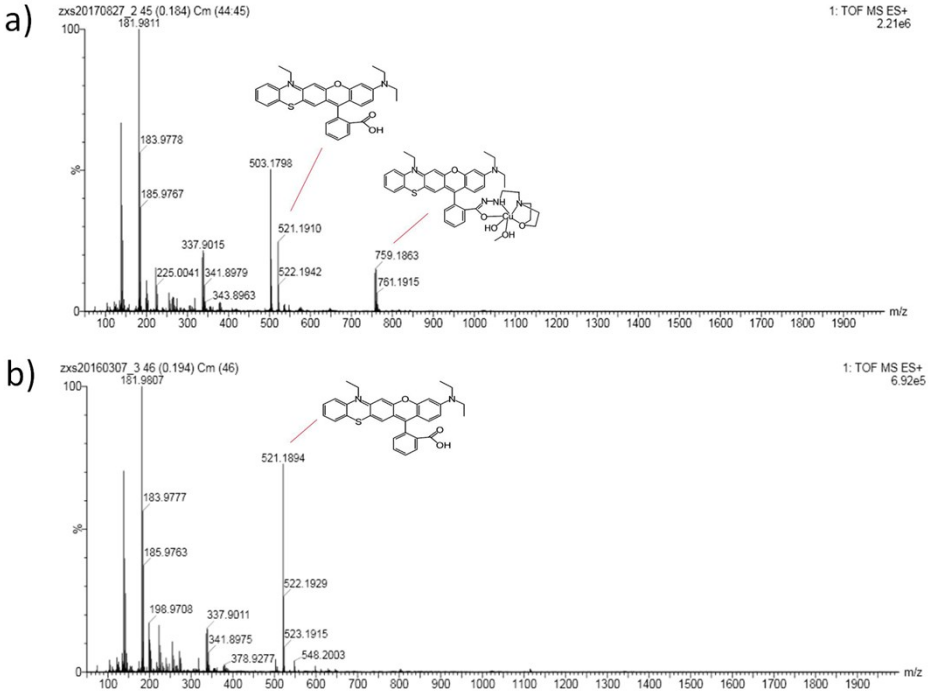

Figure S10. HRMS (LC/MS) spectra of **4** upon addition of Cu^{2+} (5.0 equiv.). a) The spectra were recorded immediately after the addition of Cu^{2+}; b) The spectra were recorded overnight after the addition of Cu^{2+}. The peak at m/z = 521.1894 was assigned to the mass of [**TJ730** + H^{+}]. The intermediate complex species (compound **4** + copper ion + OH + MeOH) can only be found after the addition of Cu^{2+} immediately, which corresponded to the peak at m/z = 759.1863 (calcd: 759.2616).

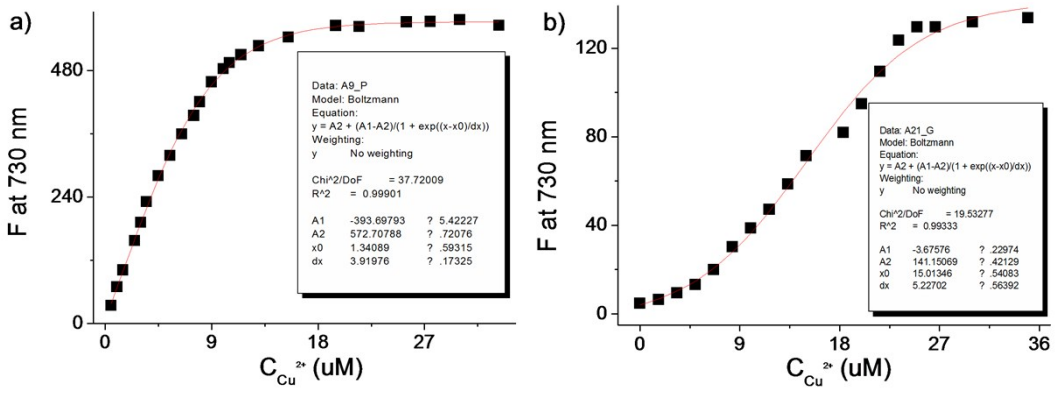

Figure S11. Measurement of the fluorescence turn-on constant ($K_{turn\text{-}on}$) of **3** and **4** (5 μM).[S2]

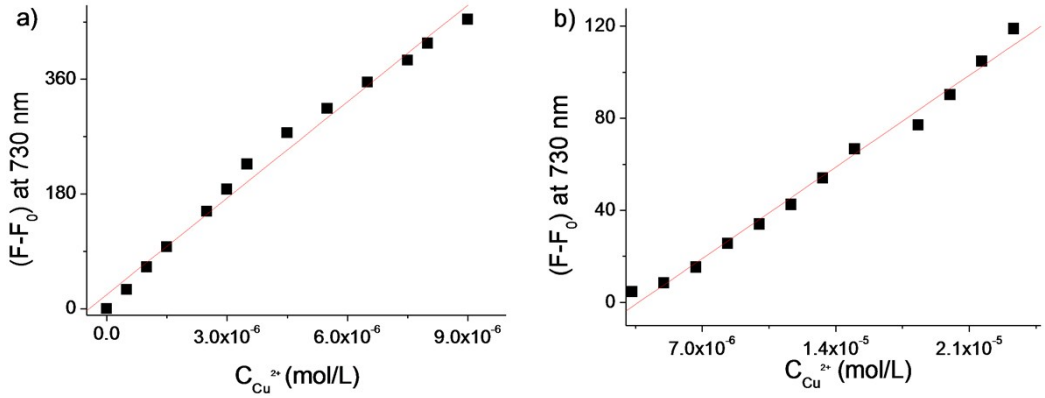

Figure S12. The fluorescence intensity change ($\Delta F = F - F_0$) versus [Cu^{2+}]. The detection limit was calculated with the following equation[S3]: Detection limit = 3σ/k Where σ is the standard deviation of fluorescence intensity of **3** and **4**, respectively; k is the slop between the fluorescence intensity change versus Cu^{2+} concentration ($k_3 = 5.046 \times 10^7$, $k_4 = 5.687 \times 10^6$). The fluorescence emission spectrum of probe **3** was measured by fifteen times and the standard deviation of blank measurement was found to be 0.0214, the detection limit is 1.3 nM. The fluorescence emission spectrum of probe **4** was measured by fifteen times and the standard deviation of blank measurement was found to be 0.0262, the detection limit is 14 nM.[S3]

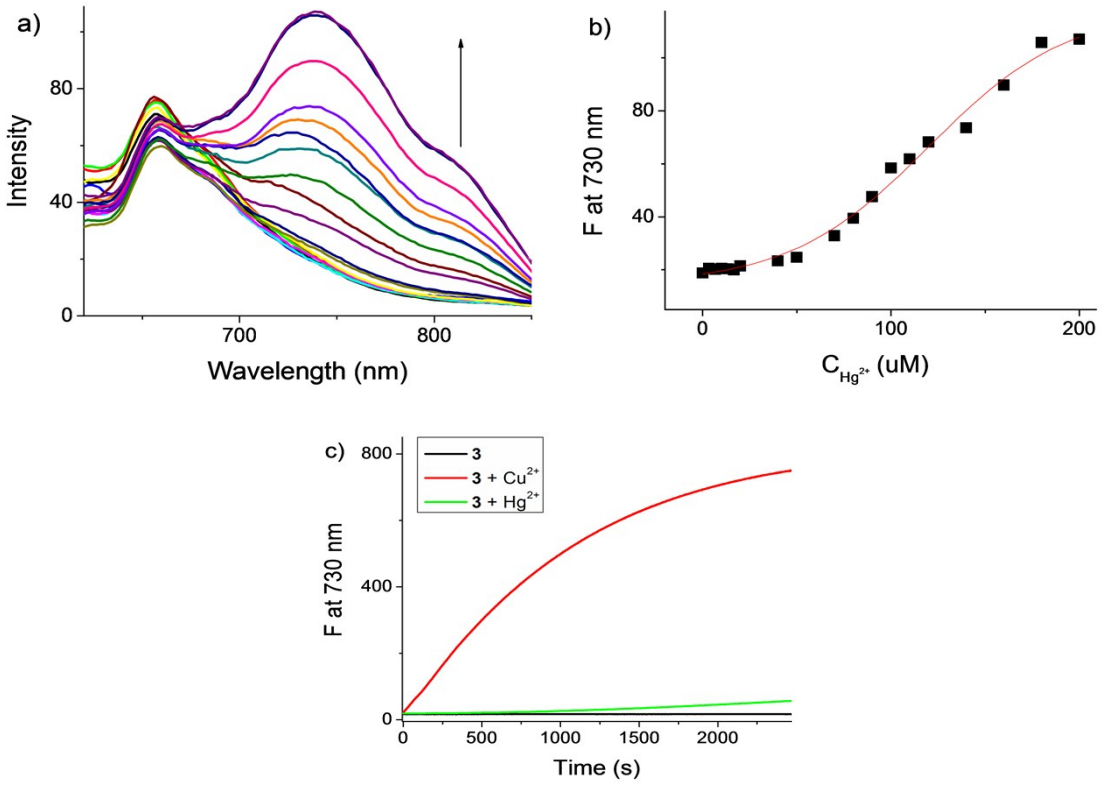

Figure S13. a) Fluorescence titrations spectra of **3** (10 μM) in the presence of different concentrations of Hg^{2+} in H_2O-MeCN (2:1, v/v); b) Measurement of the fluorescence turn-on constant ($K_{turn\text{-}on}$) of **3**; c) Time-dependent fluorescence intensity of **3** (10 μM) upon the addition of 10.0 equiv. Cu^{2+} and Hg^{2+} in H_2O-MeCN (2:1, v/v), respectively. λ_{ex} = 590 nm, slit = 10 nm, 10 nm.

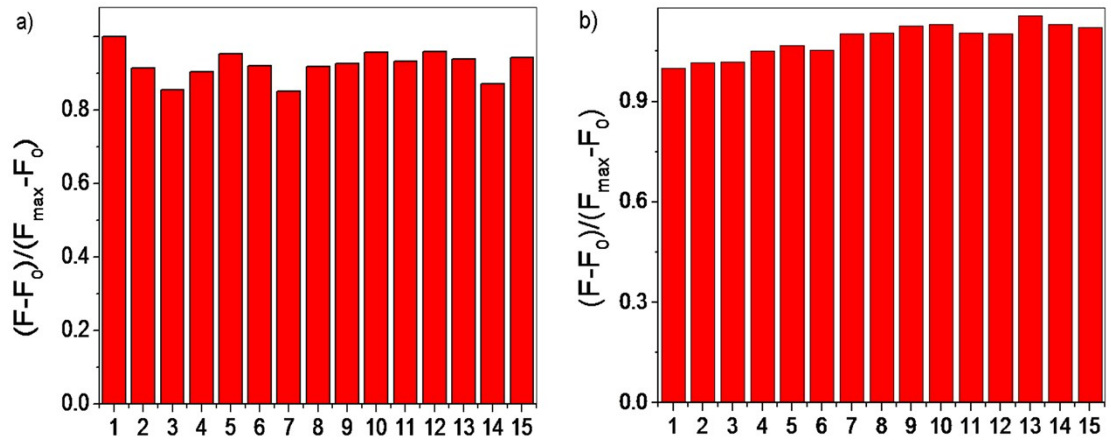

Figure S14. Change ratio $(F\text{-}F_0)/(F_{Cu^{2+}}\text{-}F_0)$ of fluorescence intensity of **3** and **4** (10 μM) at 730 nm in various mixtures of metal ions $Cu(NO_3)_2$ (50 μM) and one other metal ions (50 μM) in MeCN/water (v/v; 1/2). 1: Cu^{2+}; 2: Cu^{2+} + Ag^{+}; 3: Cu^{2+} + Al^{3+}; 4: Cu^{2+} + Ca^{2+}; 5: Cu^{2+} + Cd^{2+}; 6: Cu^{2+} + Co^{2+}; 7: Cu^{2+} + Cr^{3+}; 8: Cu^{2+} + Hg^{2+}; 9: Cu^{2+} + Fe^{3+}; 10: Cu^{2+} + K^{+}; 11: Cu^{2+} + Mg^{2+}; 12: Cu^{2+} + NH_4^{+}; 13: Cu^{2+} + Ni^{2+}; 14: Cu^{2+} + Pb^{2+}; 15: Cu^{2+} + Zn^{2+}.

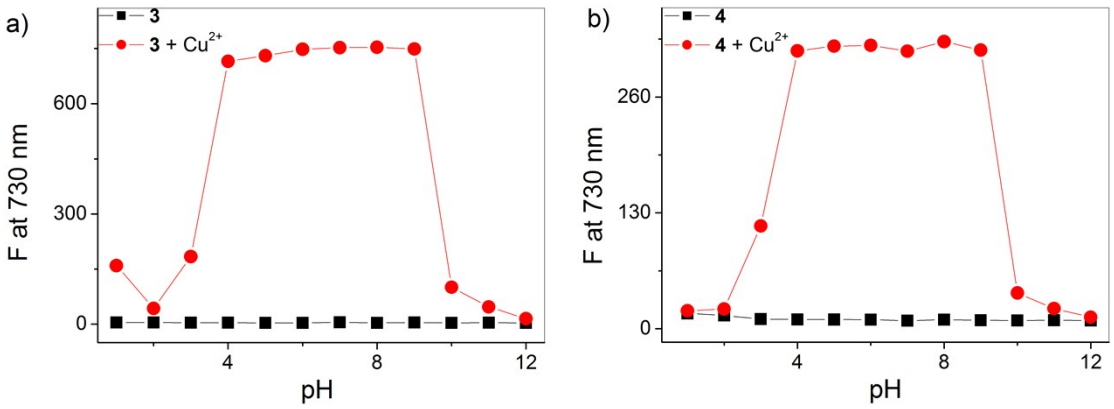

Figure S15. Fluorescence intensities of **3** and **4** (10 μM) at 730 nm in the presence and absence of Cu^{2+} (50 μM) at each pH.

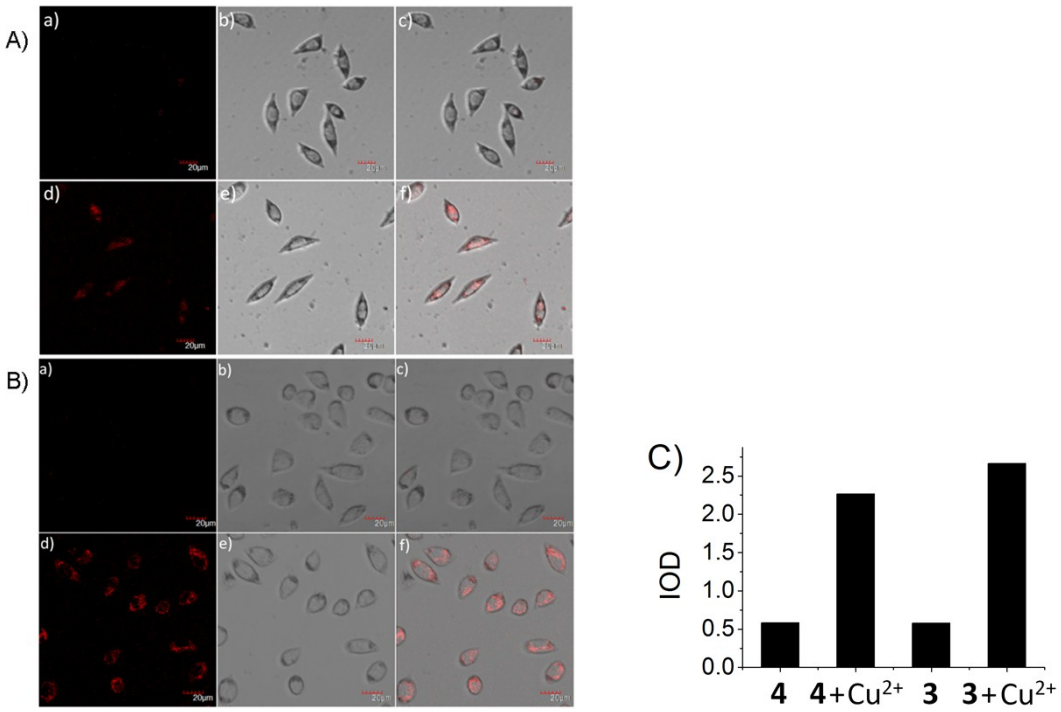

Figure S16. A) Confocal fluorescence images of **3** in living L929 cells. a) The fluorescence was collected at 647-747 nm; b) Brightfield image of live L929 cells treated with 2 μM **3** for 30 min at 37 ºC; c) Overlay of a) and b); d) The fluorescence was collected at 647-747 nm; e) Brightfield image of live L929 cells pretreated with 5 μM Cu^{2+} for 30 min at 37 ºC, then were incubated with 2 μM **3** for 30 min; f) Overlay of d) and e). B) Confocal fluorescence images of **4** in living L929 cells. a) The fluorescence was collected at 647-747 nm; b) Brightfield image of live L929 cells treated with 2 μM **4** for 30 min at 37 ºC; c) Overlay of a) and b); d) The fluorescence was collected at 647-747 nm; e) Brightfield image of live L929 cells pretreated with 5 μM Cu^{2+} for 30 min at 37 ºC, then were incubated with 2 μM **4** for 30 min; f) Overlay of d) and e). C) Histogram representing the integrated optical density (IOD) of the probe from the fluorescence images A) and B). Fluorescence images obtained according to the emission collected by the red channel (λ_{ex} = 635 nm, band path 647-747 nm).

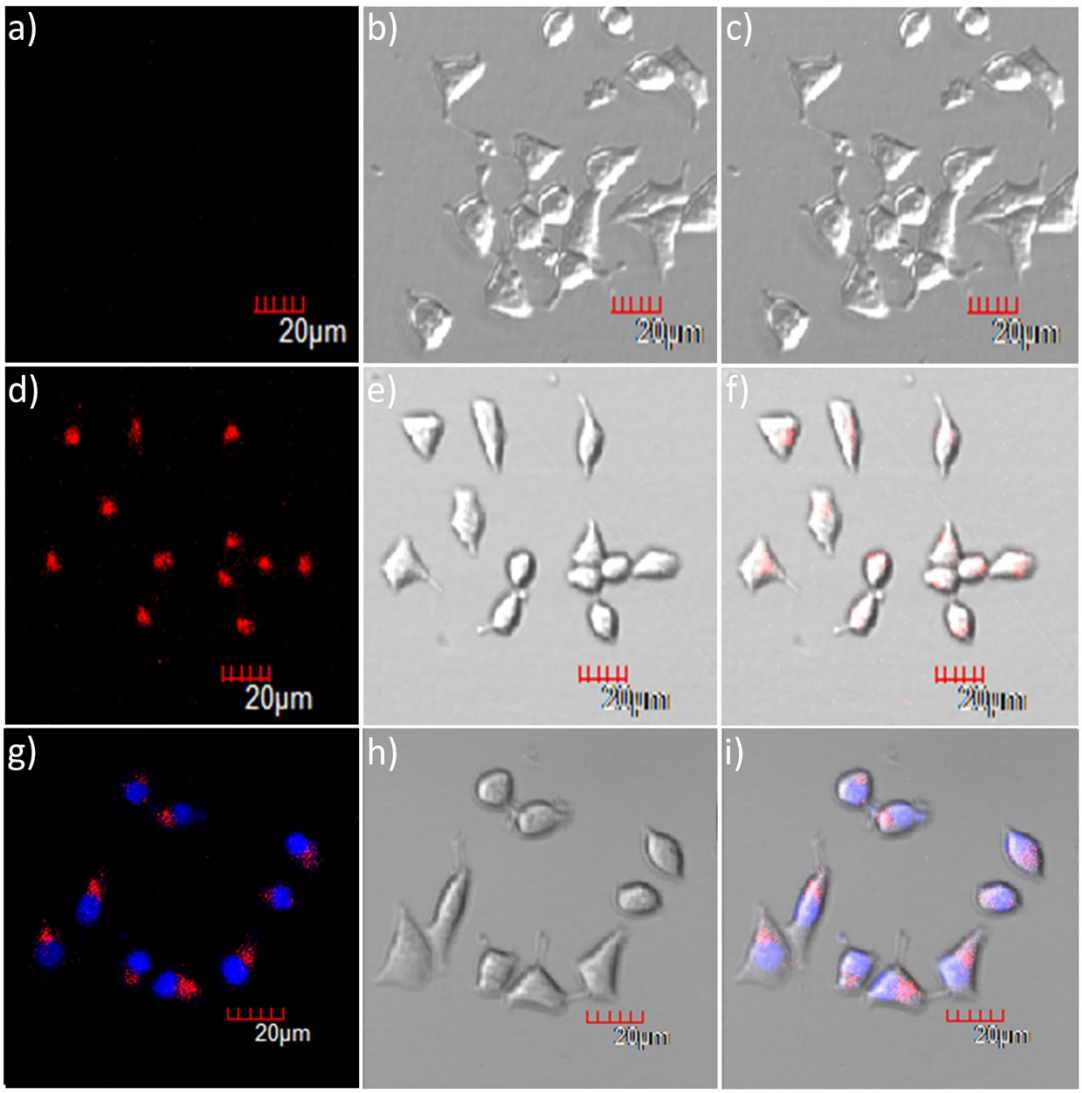

Figure S17. Confocal fluorescence images of live INS-1 cells incubated with the probe **4**. a) and b) Fluorescence and brightfield images after staining for 30 min (λ_{ex} = 635 nm, λ_{em} = 655-755 nm); c) Overlay of a) and b). d) and e) Fluorescence and brightfield images after incubated with 5 μM Cu^{2+} for 30 min; f) Overlay of d) and e); g) Overlay INS-1 cells loaded with 0.36 μM DAPI channel for 12 h and **4** (2 μM) for 30 min, and then were incubated with 5 μM Cu^{2+} for 30 min channel; h) Brightfield; i) Overlay g) and h). DAPI set: λ_{ex} = 405 nm, λ_{em} = 425-475 nm.

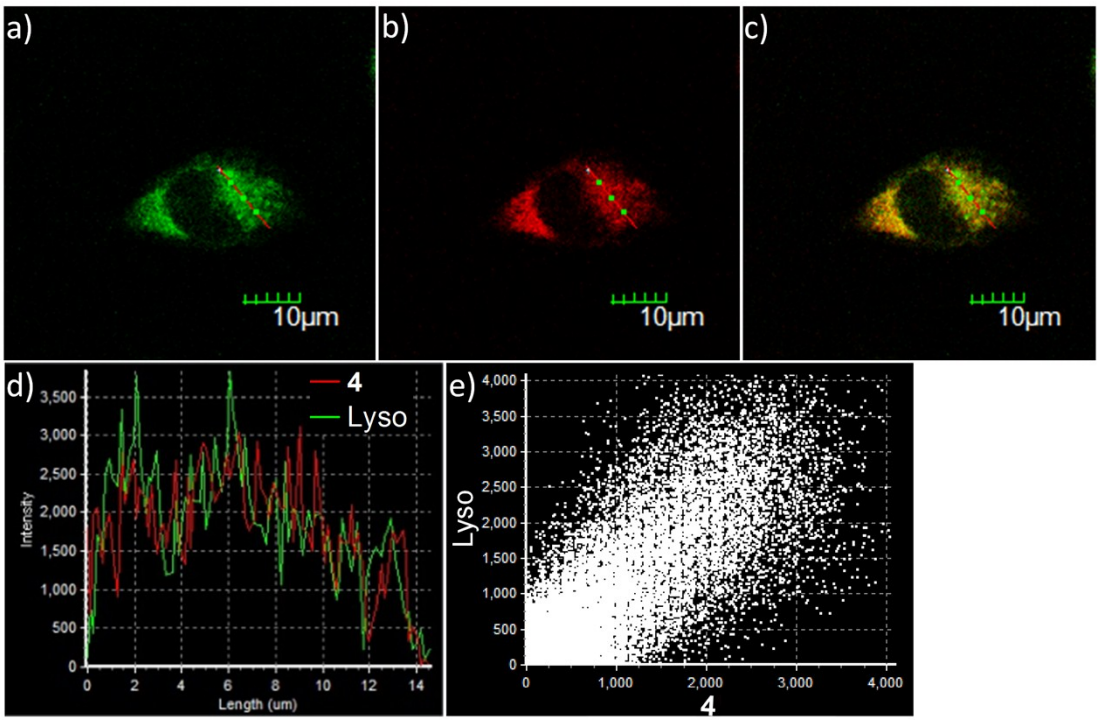

Figure S18. Colocalization of LysoTracker Green and **4** in HeLa cells. Cells were co-stained with LysoTracker Green (50 nM) and **4** (2 μM) at 37 °C for 30 min, and then treated with Cu^{2+} (5 μM) at 37 °C for another 30 min. a) Fluorescence image from the LysoTracker Green (λ_{ex} = 405 nm, λ_{em}: 507-545 nm); b) Fluorescence image from the **4** channel (λ_{ex} = 635 nm, λ_{em}: 665-765 nm); c) Merged image of images a) and b); d) Intensity profiles of LysoTracker Green and **4** within the linear ROIs (red lines in (a) and (b)) across the HeLa cells; e) Intensity correlation plot of LysoTracker Green and **4**. Green lines represent the intensity of the LysoTracker Green and red lines represent the intensity of the probe.

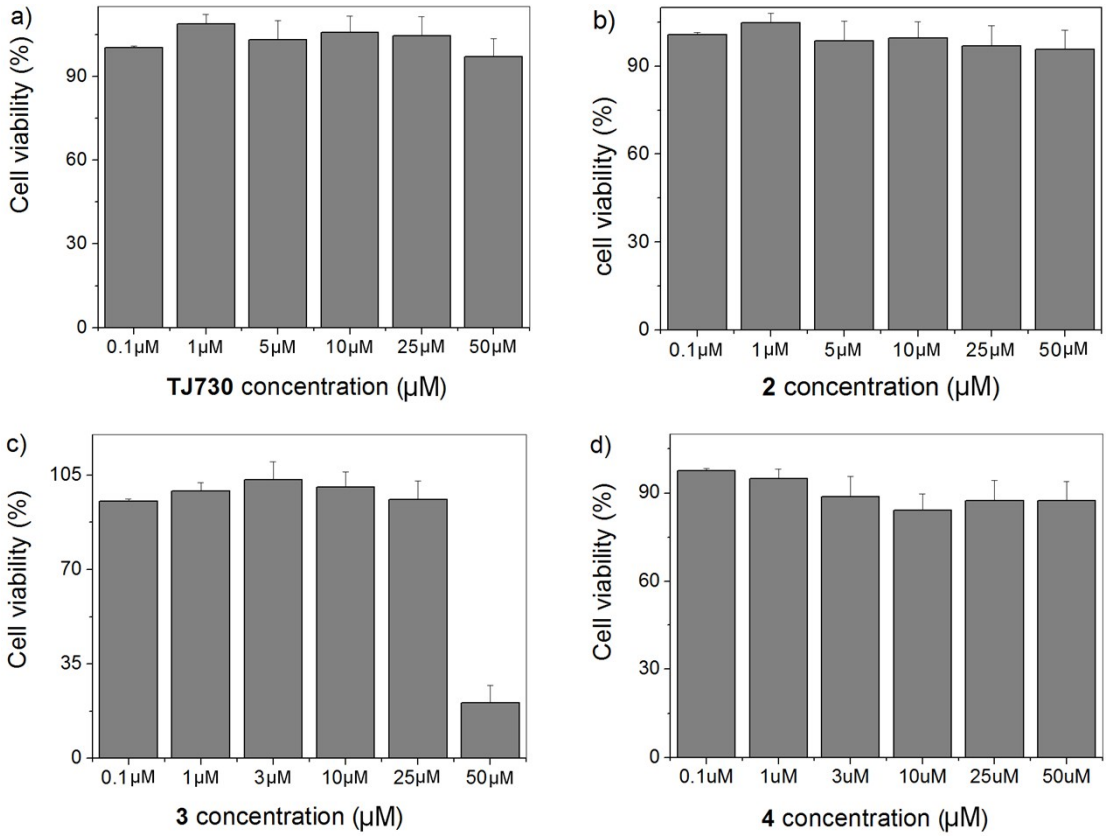

Figure S19. Effects of **TJ730** (a), **2** (b), **3** (c) and **4** (d) at varied concentrations on the viability of L929 cells after an incubation time of 24 h.

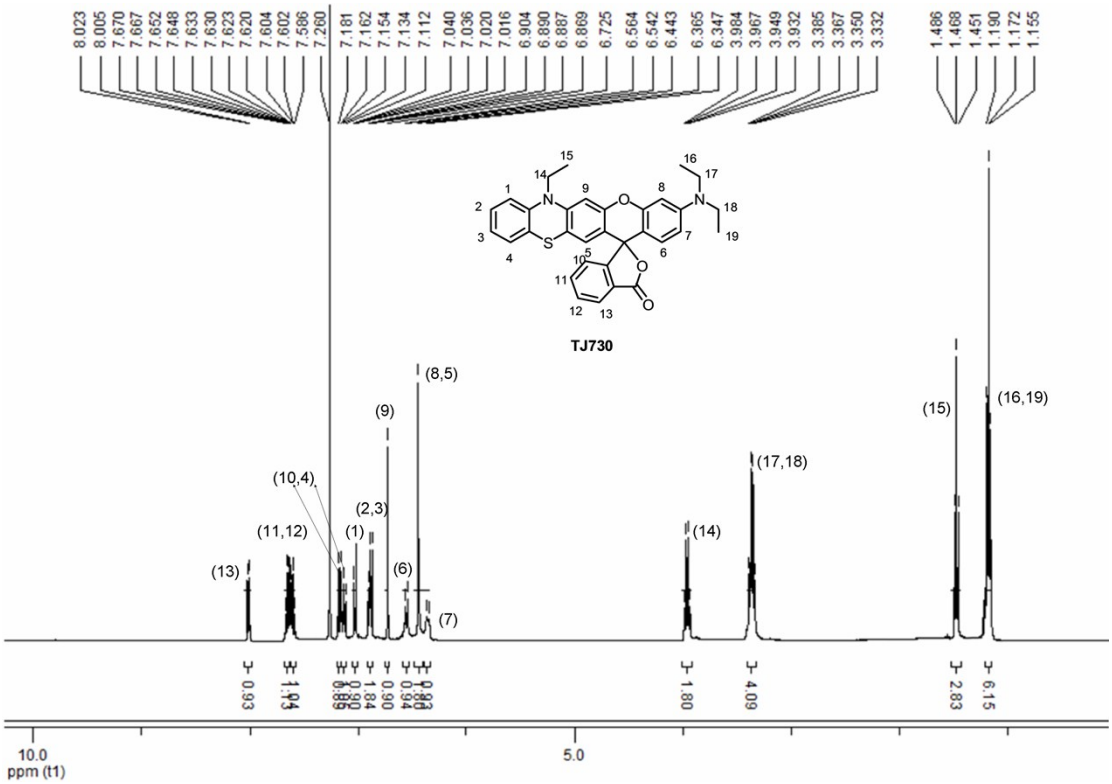

Figure S20. ^{1}H NMR of **TJ730** (400 MHz, $CDCl_3$).

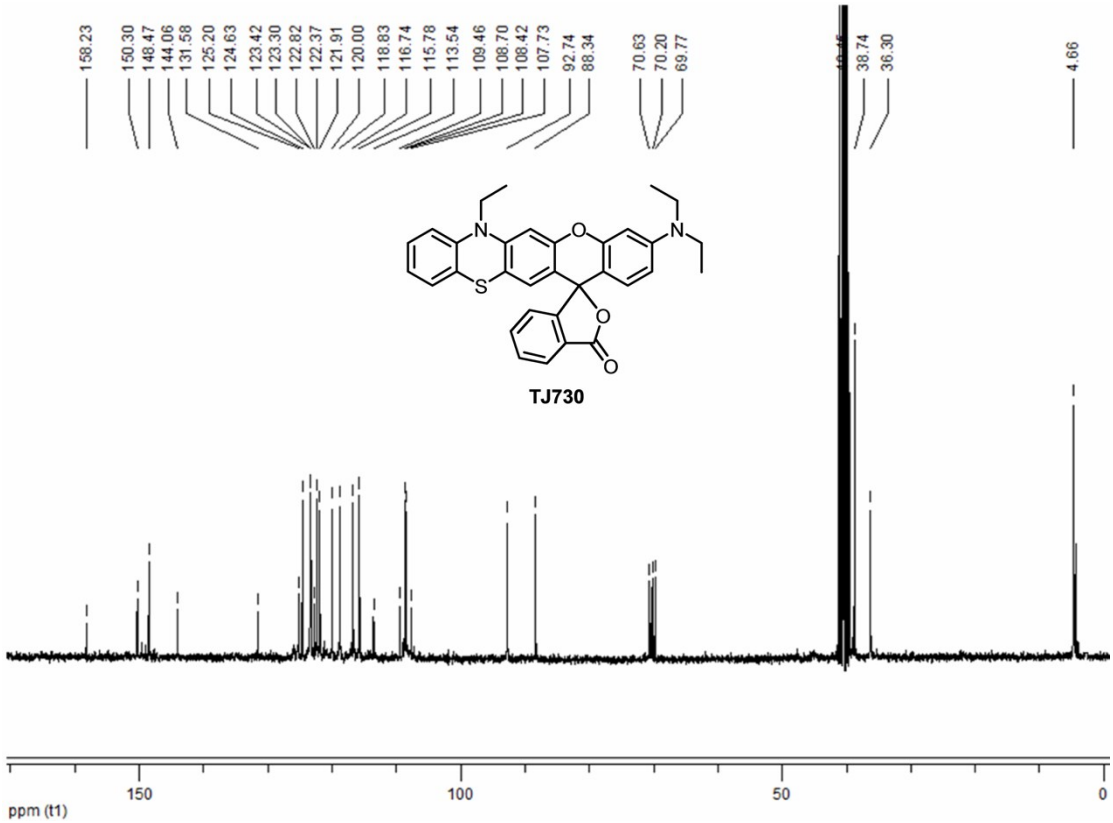

Figure S21. ^{13}C NMR of **TJ730** (100 MHz, DMSO-d_6).

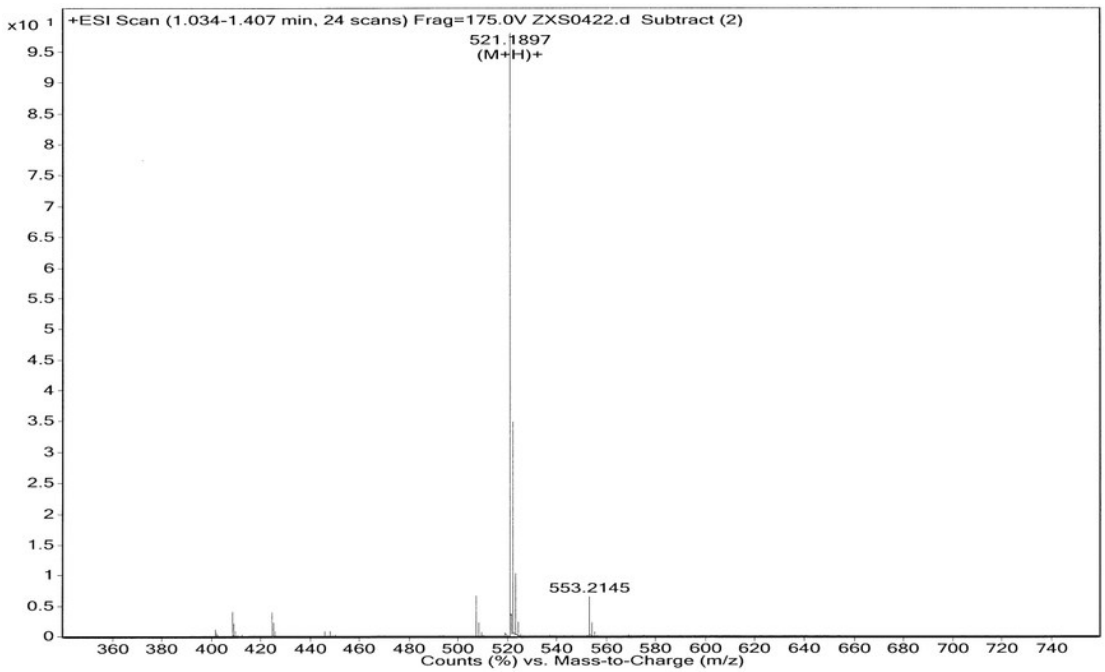

Figure S22. HRMS (LC/MS) spectra of **TJ730**. The peak at m/z = 521.1897 was assigned to the mass of [**TJ730** + H^+].

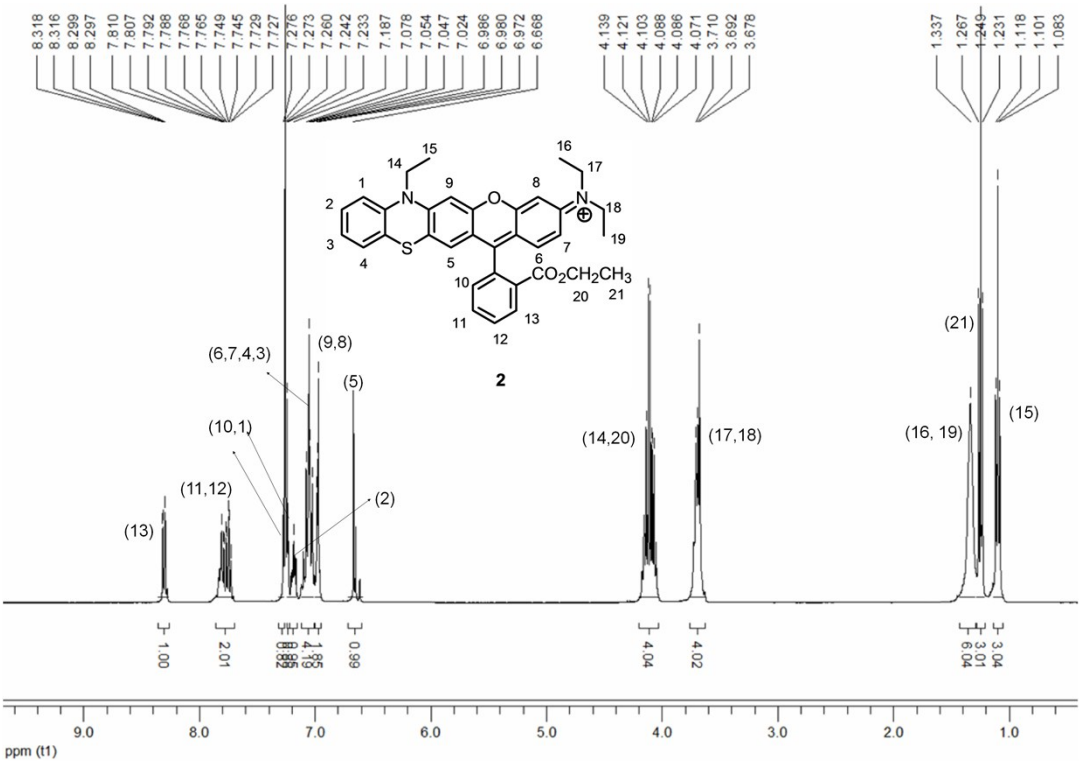

Figure S23. ^{1}H NMR of **2** (300 MHz, $CDCl_3$).

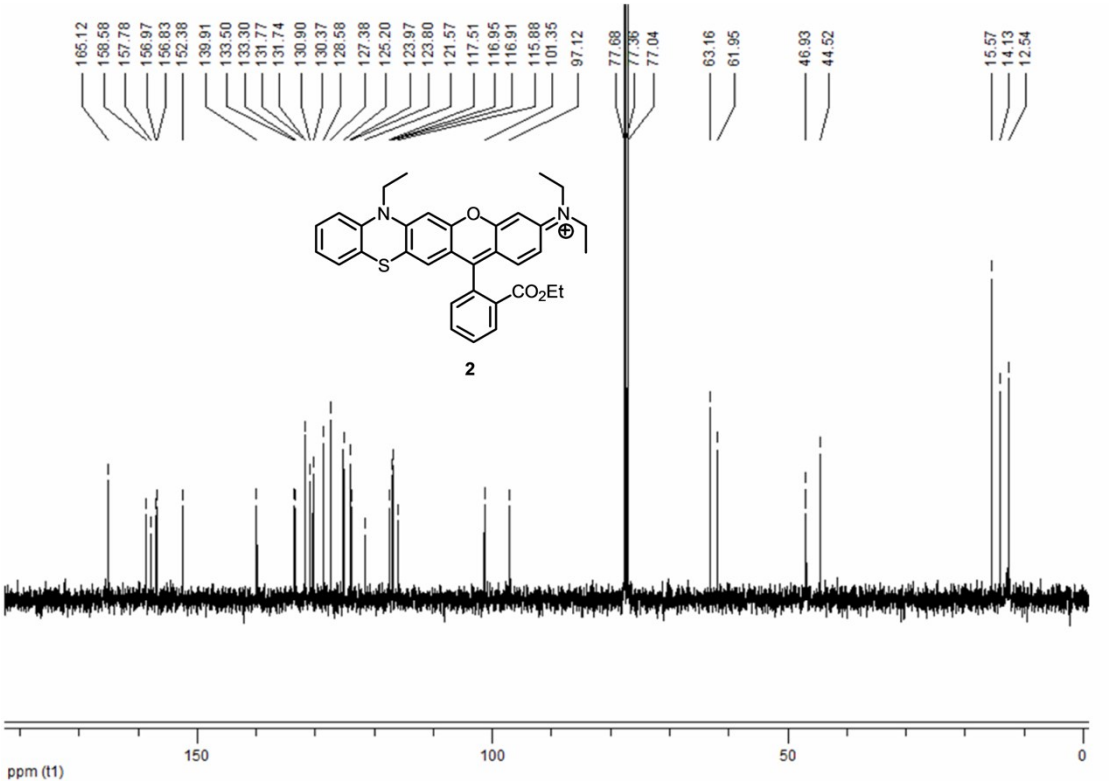

Figure S24. ^{13}C NMR of **2** (75 MHz, $CDCl_3$).

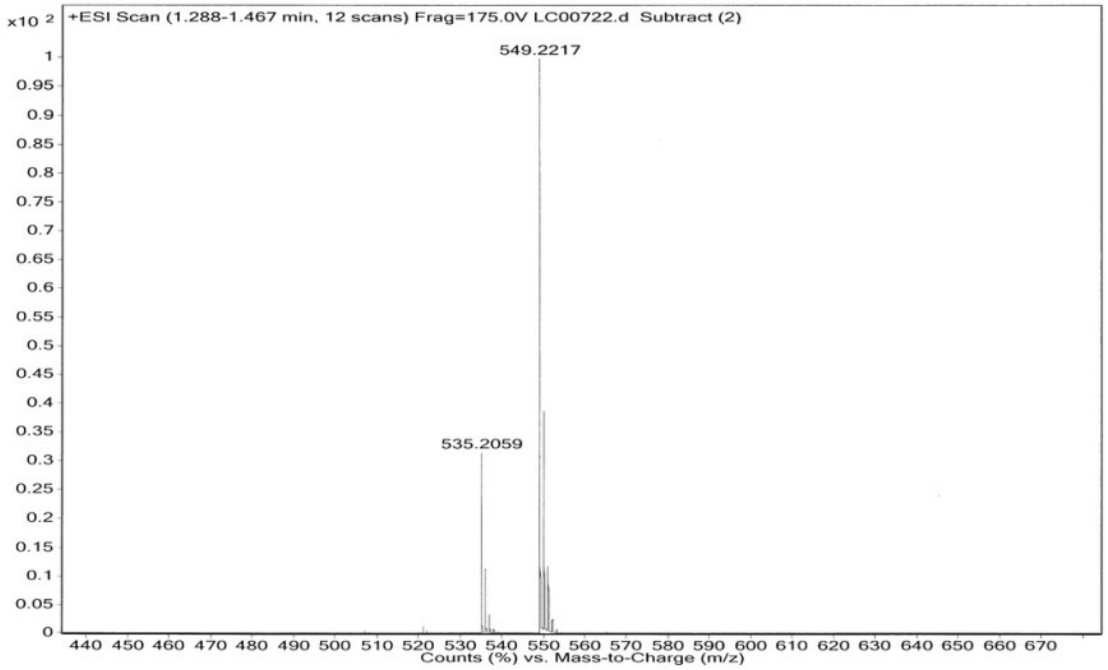

Figure S25. HRMS (LC/MS) spectra of **2**. The peak at m/z = 549.2217 was assigned to the mass of [**2** + H^+].

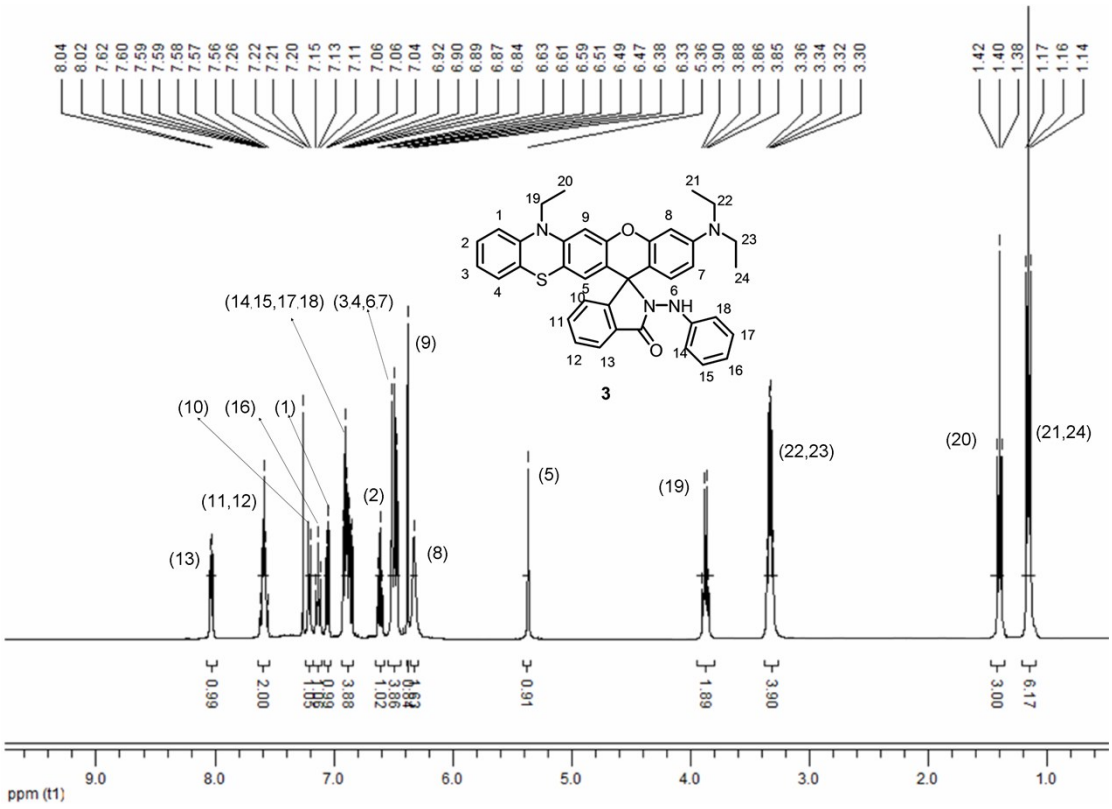

Figure S26. ^{1}H NMR of **3** (400 MHz, $CDCl_3$).

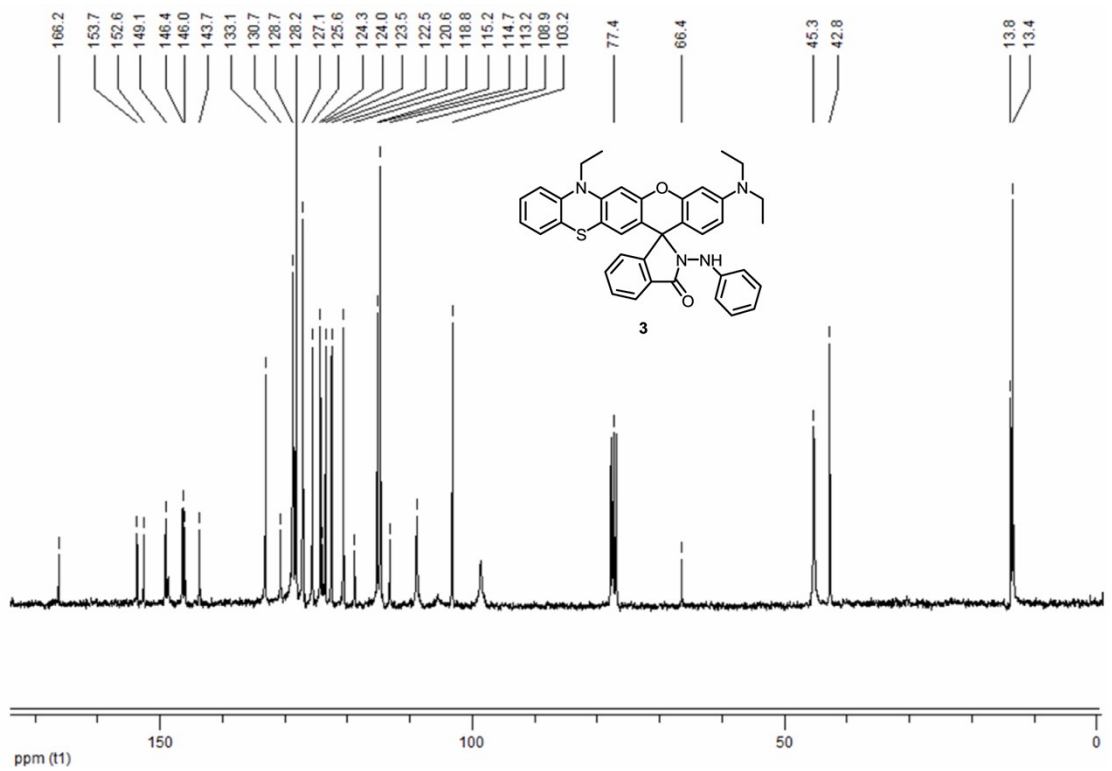

Figure S27. ^{13}C NMR of **3** (75 MHz, $CDCl_3$).

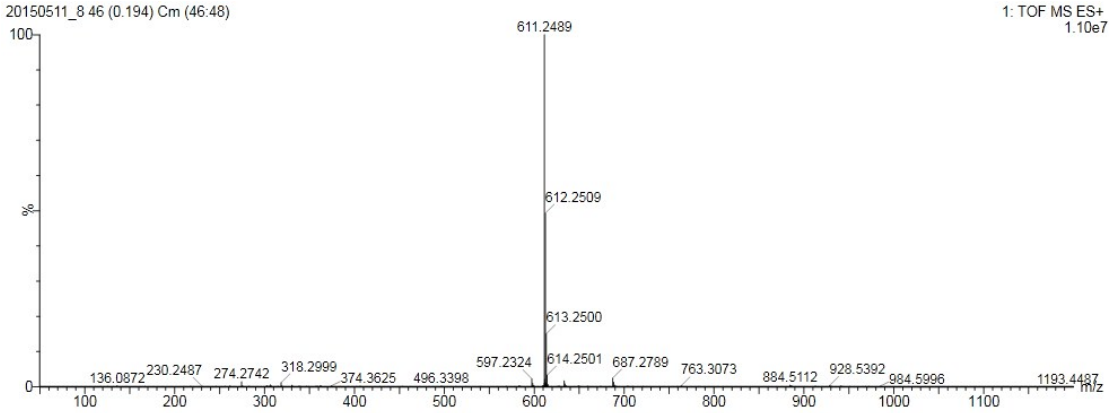

Figure S28. HRMS (LC/MS) spectra of **3**. The peak at m/z = 611.2489 was assigned to the mass of [**3** + H^+].

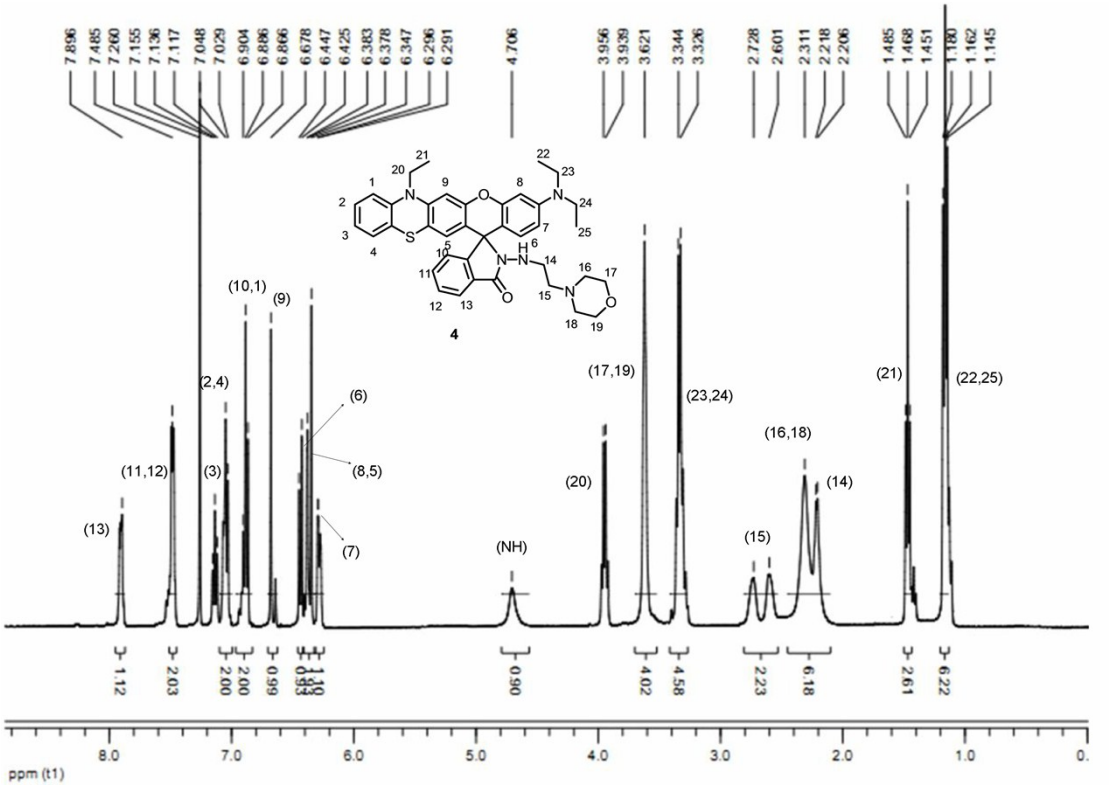

Figure S29. ^{1}H NMR of **4** (400 MHz, $CDCl_3$).

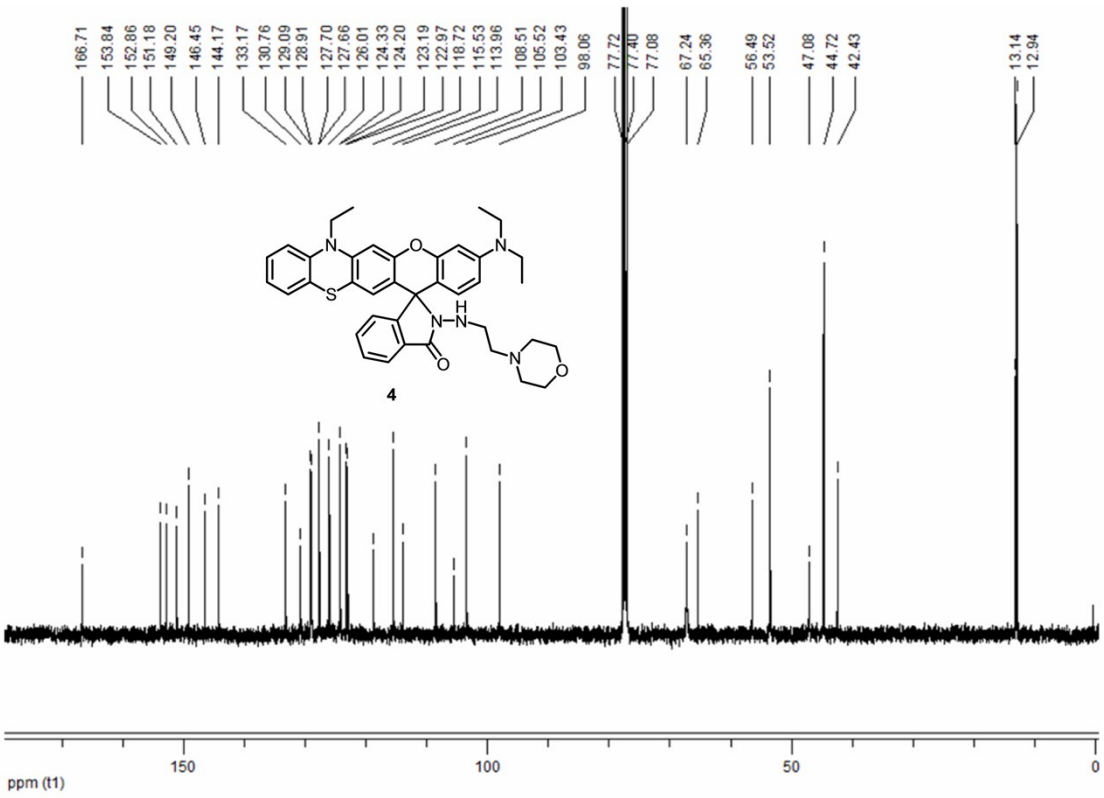

Figure S30. ^{13}C NMR of **4** (100 MHz, $CDCl_3$).

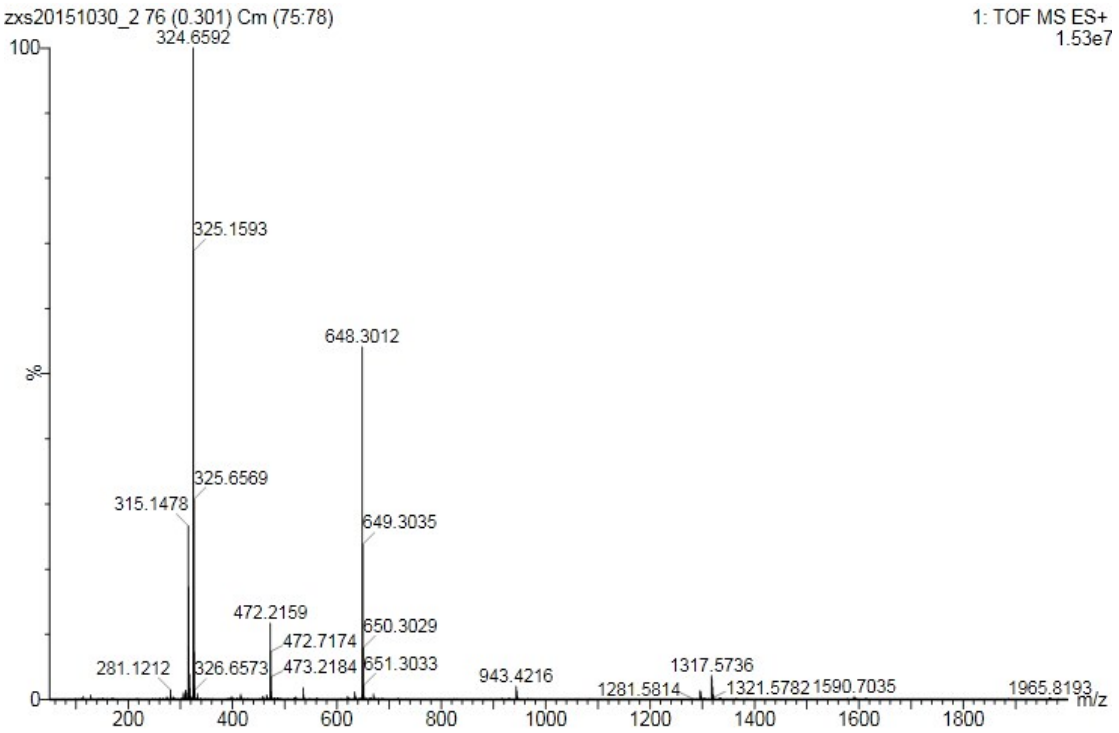

Figure S31. HRMS (LC/MS) spectra of **4**. The peak at m/z = 648.3012 was assigned to the mass of [**4** + H^+], the peak at m/z = 324.6592 was assigned to the mass of [**4** + H^+]/2.

S1. T. Karstens, K. Kobs, *J. Phys. Chem.* **1980**, *84*, 1871.
S2. P. Du, S. J. Lippard, *Inorg. Chem*. **2010**, *49*, 10753.
S3. (a) G. Long, J. Winefordner, *Anal. Chem.* **1983**, *55*, 712A;
(b) S. Pandey, A. Azam, S. Pandey, H. Chawla, *Org. Biomol. Chem.* **2009**, *7*, 269.